High Power rf Test on X-band $Mg_xCa_{1-x}TiO_3$ Based Dielectric-Loaded Accelerating Structure

C. Jing*, R. Konecny*, W. Gai*, S. H. Gold[¶], J. G. Power*, A. K. Kinkead[†], and W. Liu*

* *High Energy Physics Division, Argonne National Laboratory, Argonne, IL 60439*
[¶] *Plasma Physics Division, Naval Research Laboratory, Washington, DC 20375*
[†] *LET Corporation, Washington, DC 20007*

Abstract. In this paper, we report experimental results on a series of high-power rf tests for dielectric-loaded accelerating (DLA) structures using a high power X-band Magnicon at the Naval Research Laboratory. The dielectric material loaded into this DLA structure is a commonly used high-Q ceramic, $Mg_xCa_{1-x}TiO_3$ (MCT), with a dielectric constant of 20. The purpose of these experiments is to study high-power phenomena in the DLA structure. Two important phenomena have been observed during these experiments. First, multipactor effects are strongly dependent on the dielectric material used in the DLA structure. In this case, the multipactor-induced power absorption threshold and trend to higher power differ when MCT is used instead of alumina [1]. Second, although we did not observe dielectric breakdown in the bulk dielectric, breakdown occurred at the butt-joint between adjacent dielectric sections in the MCT structure. This occurs because of manufacturing imperfections of the joint that cause large, local field enhancements.

I. INTRODUCTION

The central motivation for using dielectric-loaded waveguides for charged particle acceleration is due to its potential for higher electric field gradient and higher material breakdown threshold than conventional metallic accelerator schemes. Significant progress has been made in the past on theoretical studies and numerical simulation of dielectric-loaded accelerating (DLA) structures and numerous articles have been published in this active field [2-7]. However, it is only relatively recently that high power experiments using either beam-driven or external rf-driven DLA structures have begun in earnest and the results reported [8-10].

In this paper, we limit our discussion to external rf-driven traveling wave DLA structures, and present some very recent experiment results.

A modular DLA structure (see Fig. 1) was tested at high power, using 11.424-GHz pulsed rf. It consists of three functional parts: the rf coupler, the tapered dielectric matching section, and the constant impedance acceleration section. In principle, the rf coupler is a modal converter that converts the dominant mode in rectangular waveguide (TE_{10} mode) to the acceleration mode in the circular waveguide (TM_{01} mode) at the rf input end and vice versa for output end. The tapered transition is used for impedance matching between the metallic circular waveguide and partially

CP737, *Advanced Accelerator Concepts: Eleventh Workshop,*
edited by Vitaly Yakimenko

dielectric-loaded acceleration section which employs a dielectric tube to slow down the microwave propagating inside the waveguide to the speed of light. The external rf pulse is injected into the rectangular waveguide port of the input coupler, through the matching section and into the accelerating section where it will transfer energy to synchronized particles and then couple out the other end. Potentially, DLA structures have a higher breakdown threshold than all-metal disk-loaded waveguide, but that threshold certainly depends on the dielectric material chosen. Therefore, we need to perform high power rf tests of various DLA structures.

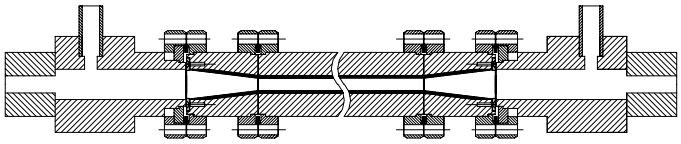

FIGURE 1. Mechanic drawing of modular DLA structure which consist of, from left to right, an all-metal TE-TM input coupler, an input tapered dielectric matching section, a constant radius dielectric accelerating section, an output tapered dielectric matching section, and an all-metal TM-TE output coupler.

The X-band Magnicon facility, developed at the Naval Research Laboratory [11], is working as an external high power 11.424-GHz rf source to feed our DLA structures. It can provide pulsed rf signals of greater than ten megawatts and less than 200 -ns pulse lengths during the experiments. Figure 2 shows the physical layout and the diagnostics used during the high power tests. The Magnicon powers the device under test (DLA structure) through WR-90 waveguide. Three bi-directional couplers with calibrated crystal detector are installed to monitor the reflected, incident and transmitted signals. Meanwhile, four ion pumps are used to monitor pressure during an arc and two cameras are used to look for visible light along the axis of the structure during an arc from both the upstream and the downstream end. The entire testing system is under vacuum at around 10^{-8} Torr.

Because of the modular configuration of the DLA structure and the broadband nature of the coupler [12], we are able use the same input and output coupler to test various DLA structures, thus reducing our fabrication cycle. We only need to redesign and fabricate different matching and acceleration pieces. In this paper, we concentrate on the testing results of a magnesium calcium titanate ceramic ($Mg_xCa_{1-x}TiO_3$, abbreviated as MCT) based DLA structure among the series of DLA structure high power rf experiment. The results from the other recent high-power test on the alumina-based structure are presented in [13]. In Section II, we begin by showing the cold test results for this MCT-based DLA structure and follow it with a presentation of the high power test results in Section III, where arcing was observed at an rf joint. In Section IV, we use an electromagnetic model to explain the results observed during the high-power tests. Finally, we propose a next generation, coaxial-type coupler to eliminate the dielectric taper section so that serious dielectric joint arcing can be avoided in the future.

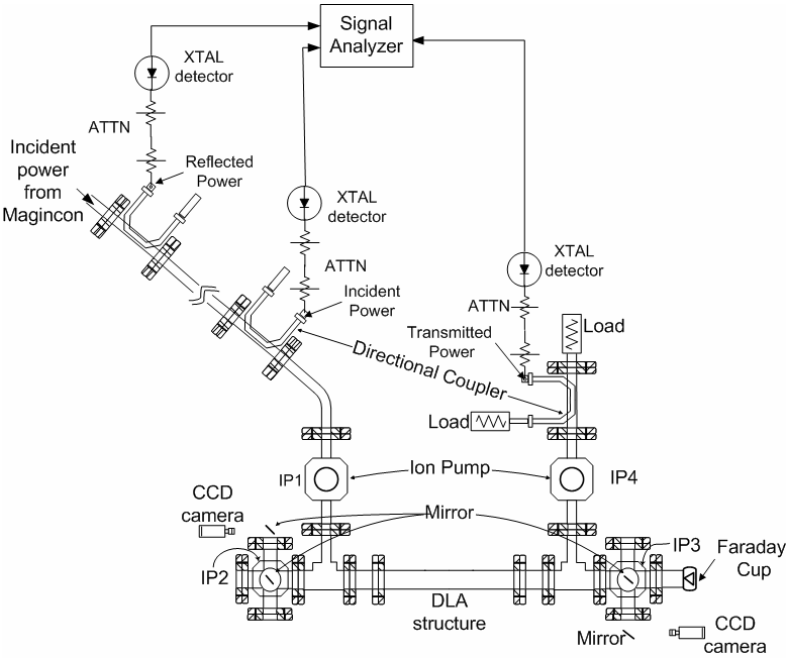

FIGURE 2. Experimental setup used to test the DLA structures with high power rf. The X-band Magnicon at the Naval Research Laboratory powered a traveling-wave dielectric-loaded accelerating structure; three bi-directional couplers were used to detect reflected, incident and transmitted power respectively; ion pumps monitored vacuum; and two CCD cameras were installed for observing arcing inside the tube.

II. BENCH TEST FOR MCT BASED DLA STRUCTURE

In general, DLA structures using high dielectric constant materials will obtain higher initial accelerating field for a given incident rf power [2]. For instance, an alumina-based DLA structure requires 80 kW of incident power while an MCT-based structure needs only 27 kW to sustain a 1 MV/m initial electric field. This is because (Table 1) MCT's dielectric constant (20) is twice as large as Alumina's (dielectric constant 9.4), and the MCT-based DLA structure has a smaller hole size.

TABLE 1. Geometric and physical properties of the 11.424GHz MCT based DLA structure.

Coefficient	Value
Material	$Mg_xCa_{1-x}TiO_3$
Dielectric Constant	20
Inner Radius	3 mm
Outer Radius	4.56 mm
Center Frequency	11.424 GHz
R over Q	8756 Ω/m
Group Velocity	0.057c

Before the high power tests at NRL, we measured the S-parameters (Fig. 3) of the DLA structure with a network analyzer at ANL. The transmission coefficient, S_{21}, is -2.4 dB and the reflection coefficient S_{11} is –10 dB at the frequency 11.427 GHz. Considering that there will be different ambient temperature and vacuum condition at NRL, these S-parameter curves will shift down a few MHz. Therefore, these bench test results are in good agreement with the high power test results (at 11.424 GHz) as shown in the next section.

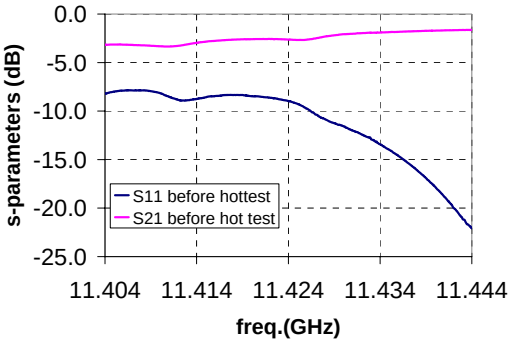

FIGURE 3. MCT DLA structure bench test results before high power rf test at the Naval Research Laboratory. Considering ambient temperature and vacuum effect, S-parameters of this DLA structure is S_{21} = -2.4 dB and S_{11} = -10 dB respectively.

III. HIGH POWER RF EXPERIMENT

We have recently finished the third series of high power rf experiments on the MCT-based DLA structure. Here, we will show the newest experimental data.

Conditioning Process

The conditioning process started after 72 hours of vacuum pumping, where the pressure was in the 10^{-8} Torr range. Characteristics of the device under test, rf power flow transmission and reflection, are shown in Fig. 4(a). The transmission curve S_{21} shows an obvious drop off when the incident rf power increases from 150 kW to 600 kW. At the same time, the reflection curve did not have a corresponding increase. Moreover, we observed diffuse, dim light during this period. All these are features of the multipactor process for the DLA structure under high power rf conditions [1, 13]. As the power was further increase, we observed some arcing around 700 kW incident power (corresponding to an accelerating gradient of 5 MV/m) and above, but no permanent damage was indicated. Limited by a tight schedule, we stopped conditioning at 1.4 MW of incident rf power (equivalent to 7.2 MV/m accelerating gradient).

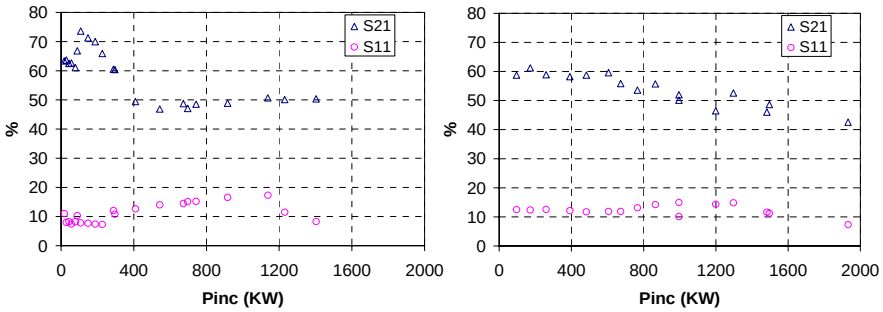

FIGURE 4. **(a)** Conditioning data for MCT-based DLA structure high power rf test. S_{21} curve does show a multipactor process during the incident power from 150 kW to 600 kW, and we observed diffuse light within this period. The arc also has been observed occasionally after incident power beyond 700 kW. **(b)** High power rf testing results of MCT-based DLA structure. Compared to conditioning data, the transmission characteristic of the tube after conditioning has changed. It may mean that the multipactor process was reduced after conditioning. Permanent arcing occurred at 1 MW rf power (6 MV/m accelerating gradient).

High Power rf testing data

After conditioning, we repeated the sweep of incident power as shown in Fig. 4(b). Interestingly, we observed a transmission curve that is different than the one from the conditioning and we didn't see multipactor light. However, we did see arcing at 1 MW of incident power. From the plot, we can see the S_{21} starts dropping at 600 kW incident power, which is much higher than seen during the conditioning process. This means the multipactor process might be being reduced by proper rf conditioning. However, we did observe a permanent arcing point at 1 MW incident power, which corresponds to 6 MV/m at the upstream end. The rf power applied to that structure was stopped at 1.9 MW due to multiple arcing spots that appeared at a dielectric joint between the upstream end taper and the uniform acceleration section, and the observation of breakdown traces on the oscilloscope.

.

IV. LOCAL FIELD ENHANCEMENT BREAKDOWN

Figure 5(a) gives us a clear image of the arcing-damaged ceramic joint. Radial dark marks show the signature of strong electron arcing. In Fig. 5(b), a typical breakdown scope trace was recorded when the incident power was raised to 1.9 MW (equivalent to over 8 MV/m accelerating gradient). At that moment, the transmitted signal was chopped off and a strong reflected signal came out during the second half of the rf pulse length.

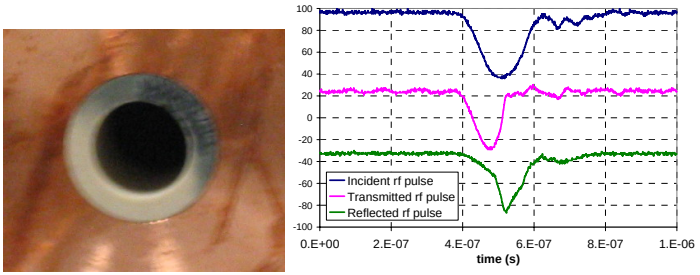

(a) (b)

FIGURE 5. (a) Dielectric breakdown signature observed at the dielectric joint between the upstream taper and the acceleration section. (b) Typical breakdown scope trace taken at 1.9 MW incident power (8 MV/m accelerating gradient).

Combined with the first two high power tests on the MCT DLA structure, we suspect that the breakdown is due to the existence of a vacuum gap in the dielectric joint. Because of the large dielectric constant discontinuity at the joint, it is expected to have a strong local field enhancement. Based on the continuity of electric flux, the local longitudinal electric field should be enhanced by 20 times compared to the normal (joint free) case. For this MCT-based DLA structure, the electric field is around 5.7 MV/m (10% power reflection considered) at the upstream end taper when 1 MW incident power applied. Then, it is estimated that over 100 MV/m E-field resides at the edge of the vacuum gap.

Using Microwave Studio® (Fig. 6), we simulated a 20 μm vacuum gap in the joint between the straight and the tapered dielectric tube near the downstream side. The numerical simulation results showed that the highest electric field exists at the gap, which is around 15 times higher than gapless case (not shown). However, it should be pointed out that this electric field enhancement could be higher due to the relatively coarse mesh applied to the simulation model (limited by our computer capability). This indirectly shows that a MCT-based dielectric-loaded accelerating structure might handle 60~80MV/m electric field without breakdown.

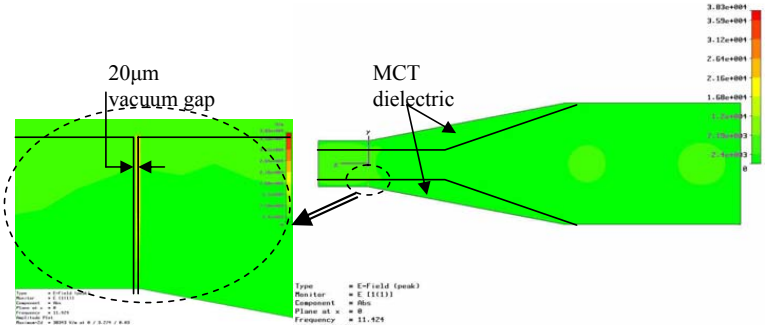

FIGURE 6. Numerical simulation demonstrates field enhancement in a small vacuum gap. From the magnified picture on the left, it shows highest the electric field built up at the small vacuum gap.

V. FUTURE WORK

From the demonstration of both EM simulation and experiment, we believe that dielectric joint related arcing is difficult to avoid in the present DLA structure. Therefore, instead of using a TE-TM converter [12] plus a dielectric taper matching section, we propose a new coaxial-type coupler which can implement TE to TM mode conversion through a TEM mode so that mode and impedance transition can be achieved simultaneously without using a tapered dielectric (Fig. 7). Simulations show that the E-field at any discontinuity inside the new coupler is very low [14], and there are no dielectric joints. Therefore, the local field enhancement in the present DLA design may be eliminated.

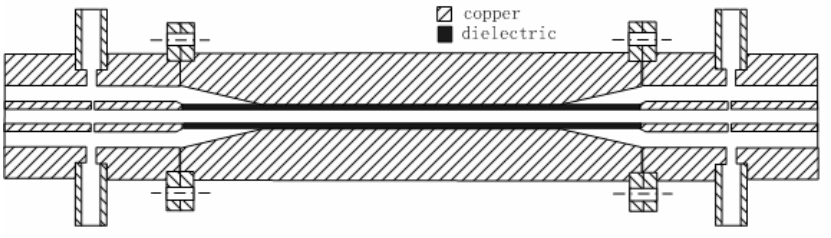

FIGURE 7. New dielectric-loaded accelerating structure design consists of two coaxial-type couplers and one dielectric-loaded accelerating section.

REFERENCES

1. J. G. Power *et al.*, *Phys. Rev. Lett*. **92**, 16 164801 (2004).
2. Peng Zou, *et al.*, *Rev. Sci. Instrum.* **71,** 2301 (2000).
3. T. B. Zhang, *et al.*, *Phys. Rev. E*, **56,** 4647 1997.
4. Wei Gai, *et al.*, *Phys. Rev. Lett.* **61,** 2756 (1988).
5. M. Rosing and W. Gai *Phys. Rev. D* **42,** 1829 (1990).
6. David Yu *et al.,* in *Advanced Accelerator Concepts: Tenth Workshop*, edited by Christopher E. Clayton and Patrick Muggli, AIP Conf. Proc. 647 (AIP, 2002) pp.484-505.
7. L. Xiao, Wei Gai, and Xiang Sun, *Phys. Rev. E*, **65**, 016505 (2001).
8. Marc E. Hill, *Phys. Rev. Lett.* **87,** 094801 (2001).
9. J. G. Power *et al,* in *Advanced Accelerator Concepts: Tenth Workshop*, edited by Christopher E. Clayton and Patrick Muggli, AIP Conf. Proc. 647 (AIP, 2002) pp.556-564.
10. D. Newsham *et al,* in *Proc. 2003 Particle Accel. Conf.,* pp.1156-1158.
11. Steven H. Gold *et al, Advanced Accelerator Concept: Tenth Workshop*, edited by Christopher E. Clayton and Patrick Muggli, AIP Conf. Proc. 647 (AIP, 2002) pp.439-447.
12. W. Liu and W. Gai, *Advanced Accelerator Concept: Tenth Workshop*, edited by Christopher E. Clayton and Patrick Muggli, AIP Conf. Proc. 647 (AIP, 2002) pp.469-475.
13. Refer to J. Power's article in this proceeding.
14. Refer to Wanming Liu's (wmliu@hep.anl.gov) EM simulation results.